Supplementary Information

A novel nanostructure to achieve ultrahigh strength and good tensile ductility of CoCrFeNiMn high entropy alloy

Yuehuang Xie [a,b], Tian Xia [a,b], Dengshan Zhou [c], Yifei Luo [a,b], Wei Zeng [a,b], Zhen Zhang [a,b], Jun Wang [a,b], Jiamiao Liang [a,b,*], Deliang Zhang [a,b,c,d,*]

[a] School of Materials Science and Engineering, Shanghai Jiao Tong University, Shanghai 200240, China

[b] Shanghai Key Lab of Advanced High-temperature Materials and Precision Forming, Shanghai Jiao Tong University, Shanghai 200240, China

[c] Key Laboratory for Anisotropy and Texture of Materials (Ministry of Education), School of Materials Science and Engineering, Northeastern University, Shenyang 110819, China

[d] Key Laboratory of Data Analytics and Optimization for Smart Industry (Ministry of Education), Northeastern University, Shenyang 110819, China

* Corresponding authors.

E-mail addresses: jmliang@sjtu.edu.cn (J.M. Liang); zhangdeliang@sjtu.edu.cn (D.L. Zhang).

Experimental details:

Elemental powders of Co, Cr, Fe, Ni, Mn (purity > 99.5 wt% and particle sizes < 75 μm) and master alloy powder of FeTi (purity > 99 wt% and particle sizes < 75 μm) were mixed (nominal composition: CoCrFeNiMn+4 at%Ti) in a planetary ball milling machine (QM-3SP4, Nanda Instrument Plant, China) at 200 rpm for 6 h and then milled at 400 rpm for 66 h with a ball to powder weight ratio of 5:1. To inhibit excessive cold welding, 0.5 wt% stearic acid was added as process control agent (PCA) and also to provide a source for C and O to form TiO(C) nanoparticles. After milling, the powder was passivated and compacted by die-pressing. Then, the compact was induction heated to 1000 °C with a holding time of 2 min, and hot extruded with the extrusion ratio of 9:1 in an argon atmosphere (named as EX). A strip with a thickness of 6 mm and width of 6.5 mm was cut from the extruded rod and forged to the thickness of 4.8 mm (~20% reduction) at liquid nitrogen temperature (the sample is named as EX+CD). Then, the strip was heat treated at 800 °C for 1h (the samples is named as EX+CD+HT).

X-ray diffraction (XRD) (D8Advance, Bruker AXS, German) with Cu kα radiation, scanning electron microscopy (SEM) (Nova 230, FEI, USA) with the back scattered electron (BSE) imaging mode, energy dispersive spectrometer (EDS) (Octane SDD, EDAX, USA), and transmission electron microscopy (TEM) (JEM 2100 and JEM 2100F, JEOL, Japan) were used to characterize the microstructure. The average grain size and nanoparticle size were estimated by image analysis using ImageJ software. In the image analysis, the sizes of the grains and nanoparticles were measured

by calculating the corresponding area-equivalent circle diameters of the grain and nanoparticle areas in the image. Due to the random distribution of the nanoparticles, their volume fraction was estimated by the area fraction on the SEM BSE images using ImageJ software.[1] The dislocation density (ρ) was calculated by the following equation[2, 3]:

$$\rho = \frac{2\sqrt{3}\,|\varepsilon|}{D_g b} \tag{S1}$$

where ε is microstrain, b is the Burgers vector (0.255 nm by XRD) and D_g is the average grain size, which can be calculated by the Williamson-Hall method based the XRD patterns by the following equation: [2, 4]

$$\beta cos\theta = \frac{0.9\lambda}{D_g} + \varepsilon sin\theta \tag{S2}$$

where β is the full width at half maximum of a diffraction at the Bragg angle of 2θ and λ is the wavelength of the X-ray. Tensile tests were conducted with dog-bone shaped specimens with gauge length, thickness and width of 12, 1 and 3 mm, respectively and using a universal testing machine (Roell Z100, Zwick, German) with a strain rate of 5×10^{-4} s^{-1}. Three tensile tests were done for each sample.

Strengthening mechanism analysis:

For metallic materials, their strength mainly depends on the mobility of dislocations and there are four main strengthening mechanisms involved in this study, as discussed below.[5] Firstly, nanoparticles can effectively strengthen metals since they become barriers for dislocation movement during plastic deformation as shown in Fig. S1(a). Nanoparticle strengthening mechanism ($\Delta\sigma_p$) can be calculated by the following Orowan equation:

$$\Delta\sigma_p = \frac{M\,\dfrac{0.4Gb}{\pi}\,\dfrac{\ln(\sqrt{\tfrac{2}{3}}D_p/b)}{\sqrt{1-\nu}}}{\sqrt{\tfrac{2}{3}}D_p\left(\sqrt{\dfrac{\pi}{4f}}-1\right)} \tag{S3}$$

where υ is the Poisson's ratio (0.26 for the CoCrFeNiMn alloy), D_p is the mean diameter of the particles and f is the particle volume fraction.[6-8] Besides, the interactions between dislocations, which can be observed in Fig. S1(b), will also cause the increasing of dislocation movement resistance.[5] This strengthening mechanism ($\Delta\sigma_d$) can be estimated by the following Taylor equation:

$$\Delta\sigma_d = \alpha MGb\sqrt{\rho} \tag{S4}$$

where α is the strength coefficient of the dislocation network, which can be taken to be 0.16, M is the Taylor factor, which can be taken to be 3.06 for FCC structure alloys, G is the shear modulus, which can be taken to be 80 GPa.[9-11] Meanwhile, grain boundaries

are also barriers for dislocation movement. In coarse grained metals, dislocations pile up at grain boundaries during plastic deformation.[11] However, it is widely accepted that theses boundaries change into the source of dislocations in ultrafine or nanoscale grained metals.[12] The extra dislocations emitted from grain boundaries increases the dislocation density, leading to the increasing of strength.[11] For grain boundary strengthening mechanism ($\Delta\sigma_g$), it can be estimated by the Hall–Petch relationship using the following equation:

$$\Delta\sigma_g = K_{HP}D_g^{-1/2} \tag{S5}$$

where K_{HP} is the Hall–Petch coefficient, which can be taken to be 490 MPa·μm$^{1/2}$.[11, 13, 14] As special grain boundaries, twin boundaries also strengthen metals. As shown in Fig. S1(c) and (d), half dislocation loops in the vicinity of twin boundaries are observed, suggesting that dislocations can bow out from these boundaries and twin boundaries become the source of dislocations like ordinary grain boundaries in ultrafine or nanoscale grained metals.[15-18] Besides, twin boundaries can serve as barriers for dislocation movement by interacting with dislocations (Fig. 5(d)-(f)) as grain boundaries in coarse grained metals.[12, 19]

 In the EX sample, the $\Delta\sigma_d$ and $\Delta\sigma_g$ are calculated to be 82 and 730 MPa, respectively. Due to the low number density of twins in this sample, the contribution of twin boundary strengthening is negligible. This means that the extra 356 MPa increase is attributed to the introducing of Ti(O)C nanoparticles by Orowan mechanism. However, the $\Delta\sigma_p$ is calculated to be 787 MPa by Eq. (S3), which is much larger than 356 MPa. This should be attributed to the interactions between grain boundary strengthening and nanoparticle strengthening. After the deformation at the cryogenic temperature, the $\Delta\sigma_d$ increases by 24 MPa calculated by Eq. (S4), while the YS of the cryogenic deformation is 207 MPa higher than that of the EX sample. The extra 183 MPa increase should be owing to the introduction of deformation nanotwin. After heat treatment, the $\Delta\sigma_g$ and $\Delta\sigma_d$ decrease to 564 and 92 MPa, respectively. Due to the stability of the Ti(O)C nanoparticles during heat treatment, the strengthening from nanoparticles can be considered unchanged, being 356 MPa. Based on them, the strengthening from nanotwin boundaries can be estimated to be 301 MPa.
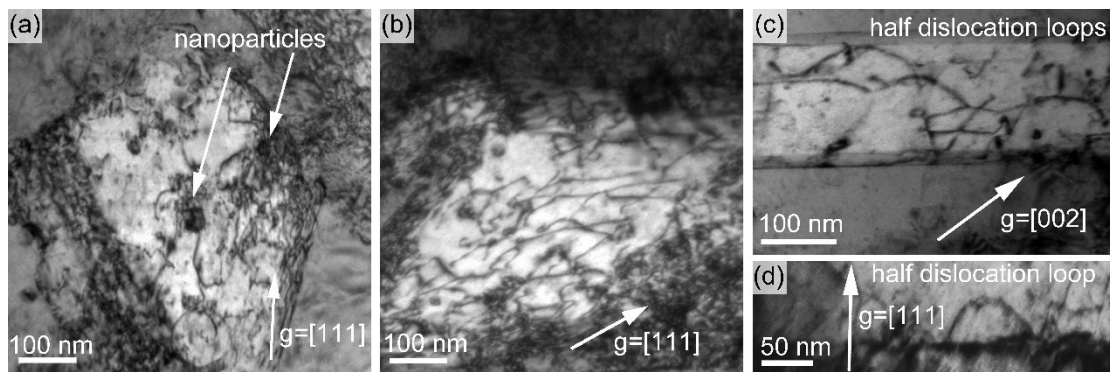
Figures

Fig. S1: TEM bright field images of the EX+CD+HT sample after tensile test under two-beam condition showing (a) dislocations pinned by the nanoparticles, (b) dislocations interacting with each other, (c) and (d) half dislocation loops in the vicinity of twin boundaries.
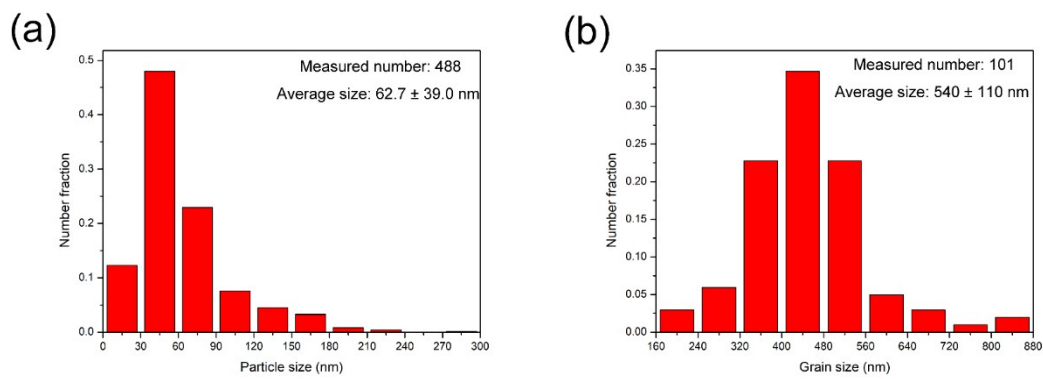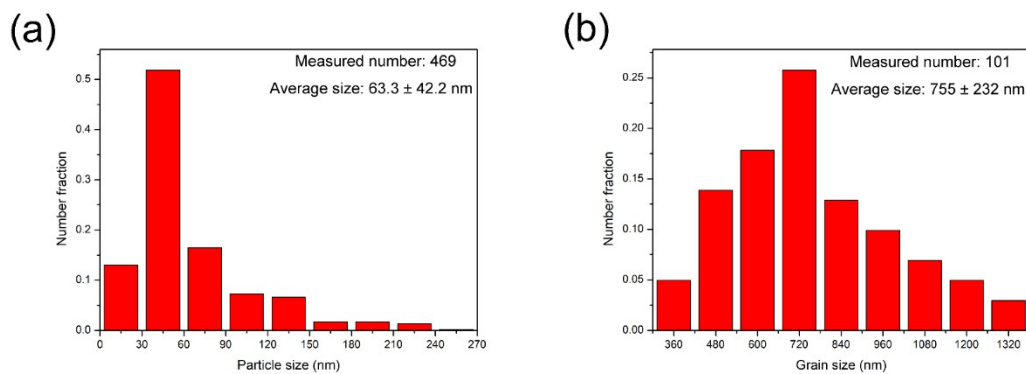

Fig. S2: (a) Particle size and (b) grain size distributions of the EX sample.
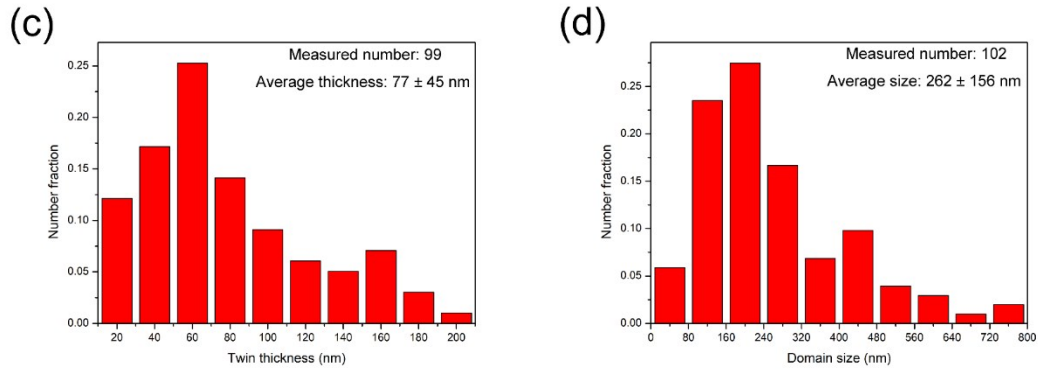
Fig. S3: (a) Particle size, (b) grain size, (c) twin thickness and (d) domain size distributions of the EX+CD+HT sample.

Reference:

1.   J. W. Martin, *Precipitation hardening: theory and applications*, Butterworth-Heinemann, 2nd edn., 1998.

2.   W. Zeng, J. Xie, D. Zhou, Z. Fu, D. Zhang and E. J. Lavernia, *J. Alloys Compd.*, 2018, **745**, 55-62.

3.   G. K. Williamson and R. E. Smallman, *Philos. Mag.*, 1956, **1**, 34-46.

4.   G. K. Williamson and W. H. Hall, *Acta Metall.*, 1953, **1**, 22-31.

5.   D.Hull and D. J. Bacon, *Introduction to Dislocations*, Elsevier, 2011.

6.   H. Wen, T. D. Topping, D. Isheim, D. N. Seidman and E. J. Lavernia, *Acta Mater.*, 2013, **61**, 2769-2782.

7.   A. Kelly and R. B. Nicholson, *Strengthening methods in crystals*, Elsevier New York, 1971.

8.   Z. Wu, H. Bei, G. M. Pharr and E. P. George, *Acta Mater.*, 2014, **81**, 428-441.

9.   Y. Xie, D. Zhou, Y. Luo, T. Xia, Z. Weng, C. Li, J. Wang, J. Liang and D. Zhang, *Mater. Charact.*, 2019, **148**, 307-316.

10.   L. Balogh, T. Ungár, Y. Zhao, Y. T. Zhu, Z. Horita, C. Xu and T. G. Langdon, *Acta Mater.*, 2008, **56**, 809-820.

11.   M. A. Meyers and K. K. Chawla., *Mechanical behavior of materials*, Cambridge university press, New York, 2nd edn., 2008.

12.   I. A. Ovid'ko, R. Z. Valiev and Y. T. Zhu, *Prog. Mater Sci.*, 2018, **94**, 462-540.

13.   S. J. Sun, Y. Z. Tian, H. R. Lin, X. G. Dong, Y. H. Wang, Z. J. Zhang and Z. F. Zhang, *Mater. Des.*, 2017, **133**, 122-127.

14.   F. Otto, A. Dlouhy, C. Somsen, H. Bei, G. Eggeler and E. P. George, *Acta Mater.*, 2013, **61**, 5743-5755.

15.   L. E. Murr and S. S. Hecker, *Scripta Metallurgica*, 1979, **13**, 167-171.

16.   K. Konopka, J. Mizera and J. W. Wyrzykowski, *J. Mater. Process. Technol.*, 2000, **99**, 255-259.

17.   A. J. Cao, Y. G. Wei and S. X. Mao, *Appl. Phys. Lett.*, 2007, **90**, 1971-1337.

18.   Y. B. Wang, B. Wu and M. L. Sui, *Appl. Phys. Lett.*, 2008, **93**, 684.

19.   L. Lu, Z. S. You and K. Lu, *Scripta Mater.*, 2012, **66**, 837-842.